Check for updates

A highly selective multi-responsive fluorescence sensor for Zn²⁺ based on a diarylethene with a 4,6-dimethylpyrimidine unit†

Xiaoxiao Wu, Zhihui Zhang, Hongliang Liu (ID)* and Shouzhi Pu*

A novel turn-on mode fluorescent diarylethene containing a 4,6-dimethylpyrimidine unit was developed to fluorescently sense Zn²⁺. Its multiple-responsive properties induced by Zn²⁺/EDTA and ultraviolet/visible light have been systematically studied. The fluorescence sensor could efficiently detect Zn²⁺ with a 10 times enhancement of emission intensity and fluorescence color change (dark-green). In addition, the sensor showed clear discrimination from Cd²⁺. The limit of detection of the sensor was measured to be 8.48×10^{-8} mol L^{-1} for Zn²⁺. Finally, a molecular logic circuit was fabricated with the emission at 528 nm as the output signal and light and chemical stimuli as input signals.
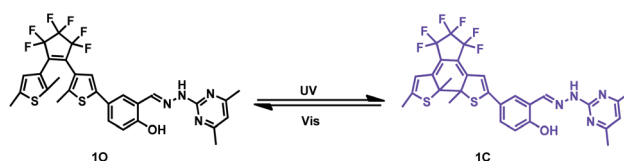
Introduction

Chemosensors are a promising research field due to the simplicity of assays, low cost and high sensitivity for metal ions in industry, medicine, biology and the environment.[1–4] In biological systems, metal ions play essential roles in different ways.[5,6] Among all the metal ions, Zn²⁺ is the second most abundant transition metal ion in biological systems and is of utmost importance for maintaining normal cellular functions, such as cell division, repair of DNA, protein synthesis, mammalian reproduction, and muscle contraction.[7–9] However, the abnormal accumulation of Zn²⁺ within the body could create serious health issues, such as myopathy, Alzheimer's disease, epileptic seizures, encephalopathy, and various cancers.[10,11] Consequently, it is highly desirable for developing effective ways for monitoring Zn²⁺,[12] which would provide an effective and promising approach to study its physiological and pathological processes.[13]

The usual detection procedures include traditional techniques, such as, chromatography, voltammetric and ion selective electrodes. However, many of these methods have their own disadvantages such as expensive instrument, insufficient sensitivity and analytes interference.[14,15] To date, much effort has been made to seek ways for detecting and tracing Zn²⁺. Among the various available techniques for sensing Zn²⁺, fluorescence detection was much more preferable, because fluorescent probes have shown many promising advantages, including high sensitivity, real-time detection, quantitative

capabilities, low cost, and easy operation.[16–18] In general, since Cd²⁺ and Zn²⁺ are in the same group of the periodic table and have similar spectral response, how to eliminate the interference of Cd²⁺ during Zn²⁺ detection is a thorny problem.[33–37] Undoubtedly, it is very important to design fluorescent sensor for the selective quantification of Zn²⁺ without interference from Cd²⁺ and other metal ions.

In order to deeply understand the crucial role of Zn²⁺ in important life processes, large amounts of Zn²⁺ fluorescent sensors have been accepted and effectively applied *in vivo*.[19–24] Among the reported fluorescent chemosensors for detecting Zn²⁺,[25–28] diarylethenes are considered one of the most potential candidates due to their remarkable fatigue resistance, excellent thermal stability, rapid response and multi-responsively photoswitchable properties under various stimulations.[29–32] To date, numerous diarylethene-based fluorescent sensors with various functional groups have been developed for the detection of Zn²⁺. Pyrimidine derivatives have gained much interest in the field of drugs, agriculture chemicals, and many biological processes. However, diarylethene-based fluorescent sensors with pyrimidine unit for detecting Zn²⁺ are relatively less known.

In this paper, we reported a novel photochromic diarylethene-based fluorescence sensor for Zn²⁺ with a 4,6-dimethylpyrimidine structure (Scheme 1). It could recognize

Jiangxi Key Laboratory of Organic Chemistry, Jiangxi Science and Technology Normal University, Nanchang 330013, PR China. E-mail: liuhongliang03@163.com; pushouzhi@tsinghua.org.cn; Fax: +86-791-83831996; Tel: +86-791-83831996

Scheme 1 Photochromism of diarylethene 1O.

Zn^{2+} with high selectivity and sensitivity through a strong blue-shift together with a remarkable fluorescence enhancement in acetonitrile solution. Furthermore, it could clearly discriminate Zn^{2+} from Cd^{2+} and other metal ions.

Experimental

General methods

All chemical reagents were provided by chemical reagent companies and used as received without further purification. The metal ions (Al^{3+}, Ca^{2+}, Pb^{2+}, Mg^{2+}, Cr^{3+}, Cd^{2+}, Mn^{2+}, Fe^{3+}, Sr^{2+}, Ag^+, Ba^{2+}, Ni^{2+}, Co^{2+} and Cu^{2+} as nitrates, and K^+, Ba^{2+}, Hg^{2+}, and Sn^{2+} as chlorides) used in metal ion selectivity experiments were dissolved in double-distilled water. EDTA solution (0.1 mol L^{-1}) was prepared with Na_2EDTA in double-distilled water. Melting point was performed on a WRS-1B melting point apparatus. ^1H NMR and ^{13}C NMR spectra were recorded on a Bruker AV400 (400 MHz) NMR spectrometer using DMSO-d_6 and CD_3CN as the solvent and chemical shifts were expressed in ppm using TMS as an internal standard. The ESI-mass spectrum was obtained using on a Bruker AmaZon SL spectrometer. The UV-vis experiments were conducted using an Agilent 8453 UV/vis spectrophotometer and the fluorescence spectra measurements were performed on a Hitachi F-4600 spectrofluorometer. Photoirradiation experiments were measured using an MUL-165 UV lamp and a MVL-210 visible lamp.

Synthesis of compound 1O

Scheme 2 shows the synthesis route of the diarylethene, 1-(2,5-dimethyl-3-thieneyl)-2-{2-methyl-5-[4-hydroxyl-3-(2-hydrazinobenzylidene-4,6-dimethylpyrimidine)-phenyl]-3-thienyl}perfluorocyclopentene (1O). The diarylethene salicylaldehyde derivative (3) was prepared by adaptation of literature procedures.[38–40]

Compound 2 (ref. 39) (3.10 g, 6.0 mmol) was cooled in dry CH_2Cl_2 at 195 K under nitrogen with vigorous stirring, followed by addition of BBr_3 (12.0 mL). The reaction mixture was stirred for 0.5 h at 195 K, and then warmed to room temperature for another 48 h. The resulting mixture was extracted with CH_2Cl_2, and then washed with water. The resulting solution was dried over Na_2SO_4. After filtration and solvent evaporation, compound 3 (0.75 g, 1.5 mmol) was well-separated *via* silica gel chromatography (eluent: petroleum ether/ethyl acetate (40 : 1)) in 35% yield. Mp 401–402 K. ^1H NMR (DMSO-d_6, 400 MHz), δ (ppm): 1.85 (s, 3H), 1.91 (s, 3H), 2.41 (s, 3H), 6.84 (s, 1H), 7.07 (d, 1H), 7.39 (s, 1H), 7.81 (d, 2H), 10.30 (s, 1H), 11.00 (s, 1H)
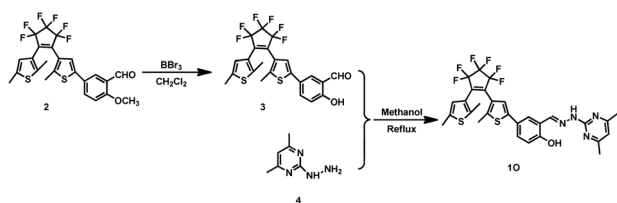
(Fig. S1†). ^{13}C NMR (DMSO-d_6, 100 MHz), δ (ppm): 13.8, 14.6, 118.2, 121.8, 122.4, 123.4, 124.2, 124.3, 125.1, 125.3, 133.1, 138.1, 139.6, 140.2, 140.6, 160.4, 190.9 (Fig. S2†). MS (ESI$^+$): m/z 503.0560 $[M + H^+]^+$ (calc. 503.0569) (Fig. S3†).

A mixture of compound 3 (0.10 g, 0.2 mmol) and 2-hydrazino-4,6-dimethylpyrimidine (4) (0.028 g, 0.2 mmol) in refluxing methanol were stirred for 6 h. Then the crude product was further recrystallized from methanol. Diarylethene 1O was obtained as a light yellow solid with a 70% yield. Mp 384–385 K. ^1H NMR (DMSO-d_6, 400 MHz), δ (ppm): 1.86 (s, 3H), 1.90 (s, 3H), 2.33 (s, 6H), 2.42 (s, 3H), 6.70 (s, 1H), 6.84 (s, 1H), 6.95 (d, 1H), 7.38 (s, 1H), 7.47 (d, 1H), 7.72 (s, 1H), 8.29 (s, 1H), 11.60 (s, 1H), 12.04 (s, 1H) (Fig. S4†). ^{13}C NMR (DMSO-d_6, 100 MHz), δ (ppm): 13.9, 14.6, 23.5, 112.1, 117.1, 119.6, 121.2, 123.5, 124.0, 124.3, 125.1, 126.0, 127.0, 138.1, 140.0, 141.5, 141.6, 157.0, 159.0, 167.6 (Fig. S5†). MS (ESI$^+$): m/z 623.1415 $[M + H^+]^+$ (calc. 623.1368) (Fig. S6†).

Results and discussion

Photochromism properties of 1O

The UV-vis spectroscopy and fluorescence changes of 1O induced by photoirradiation have been studied in CH_3CN (2.0×10^{-5} mol L^{-1}). The open-ring isomer 1O exhibited an adsorption band at 299 nm attributed to $\pi-\pi^*$ transitions at room temperature (Fig. 1A).[41] Upon ultraviolet light irradiation ($\lambda = 297$ nm), the absorption bands at 298 nm decreased and a new visible absorption band at 555 nm ($\varepsilon = 1.45 \times 10^4$ mol^{-1} L cm^{-1}) increased gradually, indicating the corresponding closed-ring isomer 1C was generated. At the same time, the photo-induced color of 1O changed from colorless to purple (Fig. 1A). A stable isosbestic point occurred at 311 nm when the photostationary state was reached, demonstrating the occurrence of a two-component photochromic reaction.[42–44] Conversely, upon visible light irradiation ($\lambda > 500$ nm), the purple closed-ring isomer 1C reverted to the colorless open-ring isomer 1O by cycloreversion reaction, and its absorption peak shifted back to 298 nm. Similar to most reported diarylethenes,[45–47] the fluorescence emission of 1O in CH_3CN also revealed the photochromic reaction occured (Fig. 1B). The open-ring isomer 1O displayed a dark yellow emission with an emission peak at 595 nm under excitation at 365 nm. Under ultraviolet light irradiation ($\lambda = 297$ nm), the emission intensity at 595 nm was gradually quenched to *ca.* 18.0% in the photostationary state due to the photocyclization product 1C generated.[48] Upon back visible light irradiation ($\lambda > 500$ nm), the emission spectra of 1C was gradually increased and recovered to the original state of 1O. In addition, the fatigue resistance of 1O was also determined by alternating irradiation of ultraviolet and visible lights at room temperature. Undergo 18 times of the coloration–decoloration cycle, the emission intensity of 1O was degraded by only 10%, as illustrated in Fig. 1C.

Spectral response of Zn^{2+}

As shown in Fig. 2, the fluorescence selectivity of sensor 1O toward 18 different various metal ions (Zn^{2+}, Al^{3+}, Ca^{2+}, Sn^{2+}, K^+,
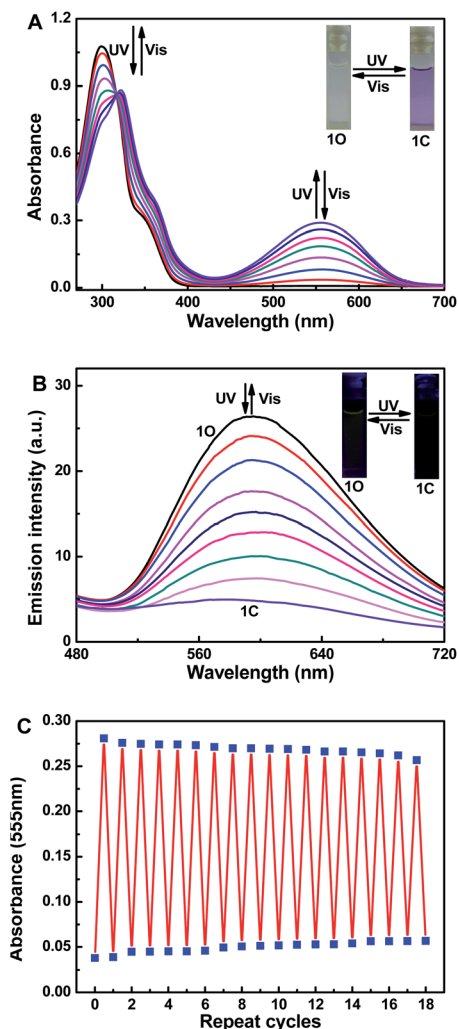

Scheme 2 Synthetic route of diarylethene 1O.

Fig. 1 Changes in the absorption and fluorescence spectra of **1O** upon alternating irradiation with UV and visible light in CH$_3$CN (2.0 × 10^{-5} mol L^{-1}): (A) absorption spectral changes; (B) fluorescence changes, excited at 365 nm; (C) fatigue resistance.

Pb^{2+}, Mg^{2+}, Cr^{3+}, Cd^{2+}, Hg^{2+}, Mn^{2+}, Fe^{3+}, Sr^{2+}, Ag$^+$, Ba^{2+}, Ni^{2+}, Co^{2+} and Cu^{2+}) was studied in CH$_3$CN (2.0 × 10^{-5} mol L^{-1}). As illustrated in Fig. 2A, **1O** exhibited a weak fluorescence emission at 595 nm. Upon addition 1 equiv. of Zn^{2+}, the fluorescence emission peak of **1O** showed a dramatic enhancement by 10 times and blue-shifted to shorter wavelength region at 528 nm due to the complex **1O–Zn^{2+}** (**1O′**) form (Fig. 2A and B). The apparent fluorescence emission color varied from dark yellow to bright green (Fig. 2C). However, upon individual addition of other metal ions, they showed no obvious fluorescence variations except Al^{3+}. Although a weak fluorescence response of **1O** toward Al^{3+} was also observed, the emission intensity was increased less than 3 folds and the dark green fluorescence color of **1O–Al^{3+}** (540 nm) was distinguishable from **1O–Zn^{2+}**. Moreover, it is noteworthy that there was no interference of Cd^{2+} (Fig. 2B), indicating high selectivity of Zn^{2+}. These data demonstrated the high selectivity of sensor **1O** toward Zn^{2+}.

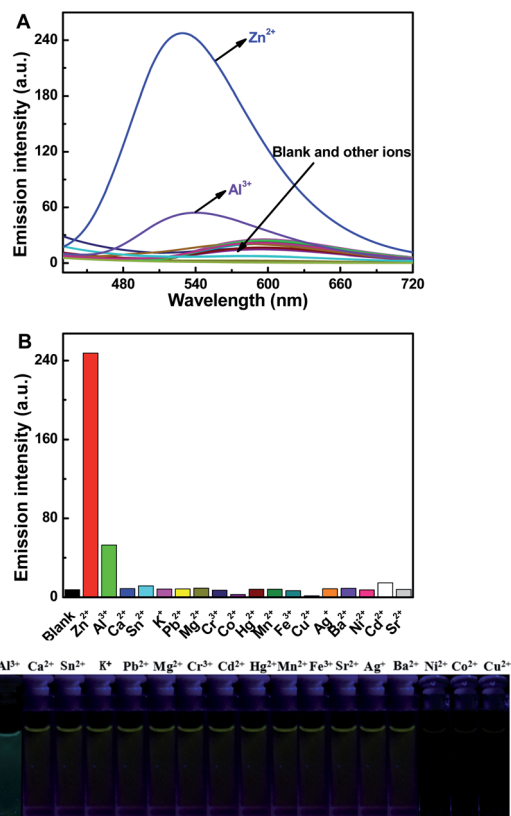The absorption spectra response of sensor **1O** induced by Zn^{2+} and ultraviolet/visible lights in CH$_3$CN was also

Fig. 2 Changes in the fluorescence of **1O** induced by various metal ions (0.6 equiv.) in CH$_3$CN (2.0 × 10^{-5} mol L^{-1}), excited at 365 nm: (A) emission spectral changes; (B) emission intensity; (C) photos of fluorescence changes in CH$_3$CN.

investigated (Fig. 3). As shown in Fig. 3A, the absorption peak of **1O** at 299 nm decreased when increasing concentrations of Zn^{2+}, and a new absorption peak at 412 nm gradually increased due to the formation of complex **1O′** (Fig. 3A). With the addition of Zn^{2+}, the solution color varied from colorless to light yellow. As shown in Fig. 3B, a dramatic absorption enhancement at 412 nm was found upon gradual addition of Zn^{2+} (0 to 9 equiv.) to **1O** solution. And the absorption intensity reached a plateau when 2 equiv. of Zn^{2+} was added. Upon ultraviolet light irradiation (λ = 297 nm), a new absorption peak of complex **1O′** at 570 nm (ε = 2.33 × 10^4 mol^{-1} L cm^{-1}) appeared and increased due to the formation of the closed-ring isomer **1C′** (**1C–Zn^{2+}** complex).[49] At the same time, a visual color varied from light yellow to dark purple was observed (Fig. 3C). Upon the addition of Zn^{2+}, the absorption intensity of **1C** at 555 nm enhanced gradually with a moderate red shift (15 nm), indicating complex **1C′** formation (Fig. 3D). However, as shown in Fig. 3A and D, on addition excess EDTA to **1O′** and **1C′** solution, the absorption spectra of **1O** and **1C** could not be restored, respectively. The result elucidated that two isomers of **1** had large affinity for Zn^{2+} and readily competes with EDTA for Zn^{2+} resulting in the irreversible response of **1O** and **1C** to Zn^{2+}.[50] In general, in order to detect metal ions, chemosensors bind with the target metal ions through non-covalent interactions to yield stable coordination complexes.[51] The Zn^{2+} ion should have a stronger binding
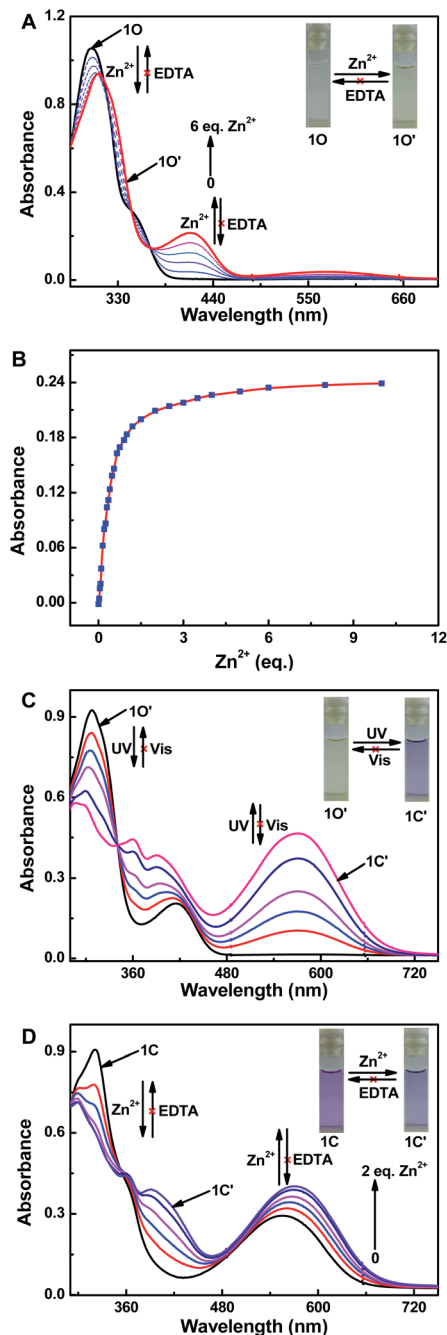
Fig. 3 Changes in the absorption spectrum and color of **1O** and **1C** induced by Zn²⁺/EDTA and light stimuli in acetonitrile (2.0 × 10⁻⁵ mol L⁻¹): (A) **1O** induced by Zn²⁺/EDTA; (B) the changes of absorbance at 412 nm with the addition of different equivalents of Zn²⁺; (C) **1O′** upon irradiation with UV/vis light.; (D) **1C** induced by Zn²⁺/EDTA.

Fig. 4 Changes in the fluorescence and color of **1O** and **1O′** induced by Zn²⁺/EDTA and light stimuli in CH₃CN (2.0 × 10⁻⁵ mol L⁻¹): (A) **1O** induced by Zn²⁺/EDTA; (B) The changes of fluorescence intensity at 528 nm with the addition of different equivalents of Zn²⁺; (C) **1O′** upon irradiation with UV/vis light.

energy to the sensor **1** than EDTA. The stronger affinity of sensor **1** to Zn²⁺ can not be reversed by EDTA.

To further elucidate the sensing behavior of **1O** for Zn²⁺ detection, we carried out the fluorescence titration test with Zn²⁺ (Fig. 4). When increasing concentrations of Zn²⁺ (0 to 1.5 equiv.), the fluorescence intensity of **1O** at 595 nm increased gradually accompanied by an obvious red-shift of 67 nm
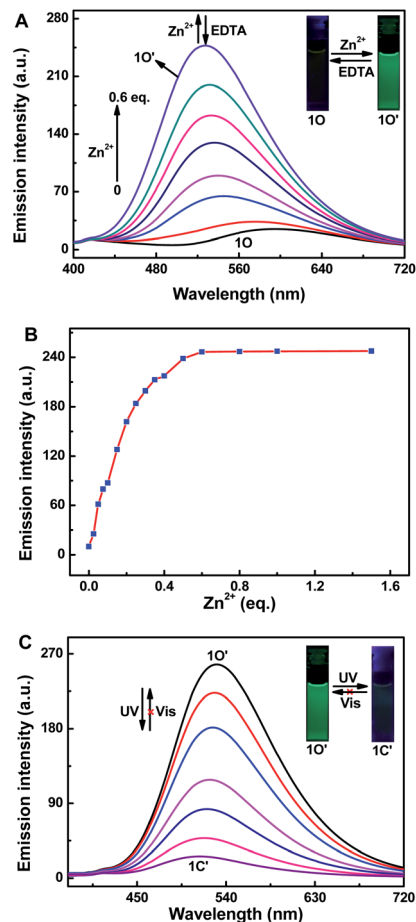
(Fig. 4A). And the fluorescence intensity reached a plateau until the concentration of Zn²⁺ reached 1 equiv. The fluorescence enhancement displayed good linearity in the Zn²⁺ concentration range 0–12 μM (Fig. 4B). Upon ultraviolet light irradiation ($\lambda = 297$ nm), the fluorescence intensity of complex **1O′** nm was gradually quenched to *ca.* 18.0% in the photostationary state due to the closed-ring isomer **1C′** generated, and a concomitant color varied from bright green to dark green (Fig. 4C). As shown in Fig. S7,† the fluorometric titration of **1C** by Zn²⁺ was also tested. Sensor **1C** displayed emission peak at 595 nm, a blue-shift by 77 nm and increased fluorescence intensity (∼10 folds) were observed with increasing concentrations of Zn²⁺. At the same time, the fluorescent color varied from dark to dark green.

Job's plot analysis was used to estimate the binding parameters of **1O** with Zn²⁺.[52] When the mole ratio of (**1O**)/[(**1O**) + (Zn²⁺)] appeared at 0.5, the maximum emission intensity of **1O′** at 528 nm was observed, indicating a 1 : 1 complexation stoichiometry of **1O** with Zn²⁺ (Fig. 5A). The association constant (K_a) of the **1O**–Zn²⁺ complex was measured as 1.72 × 10⁵ L mol⁻¹ using Benesi–Hildebrand analysis (Fig. 5B).[53] Additionally, the fluorescence sensor **1O** provided a low Zn²⁺
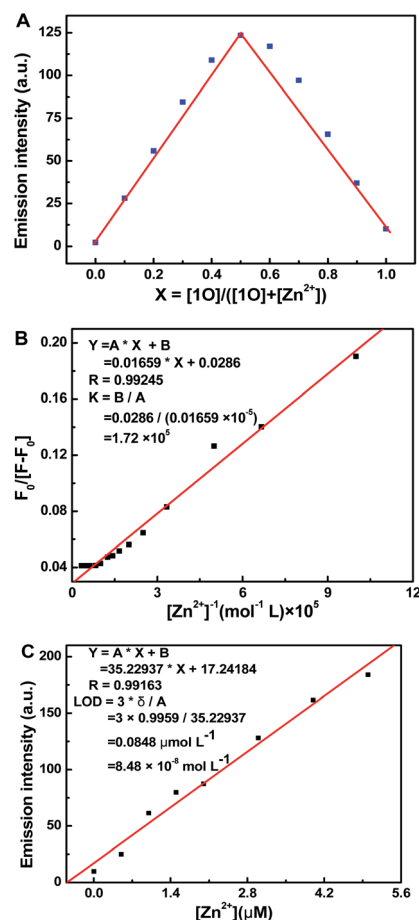
Fig. 5 Job's plot, Hildebrand–Benesi plot and the limit of detection (LOD) for **1O** in CH_3CN (2.0×10^{-5} mol L^{-1}): (A) Job's plot showing the 1 : 1 complex of **1O** and Zn^{2+}; (B) Hildebrand–Benesi plot based on the 1 : 1 for **1O**, the binding constant of **1O** with Zn^{2+} was calculated to be 1.72×10^5 L mol^{-1}; (C) LOD for Zn^{2+} is 8.48×10^{-8} mol L^{-1}.

fluorescence detection limit of 8.48×10^{-8} mol L^{-1} (Fig. 5C),[54] which was much lower than the maximum contaminant level (76 μmol L^{-1}) for Zn^{2+} in drinking water set by in the WHO. To further confirm the preferential selectivity of the fluorescence
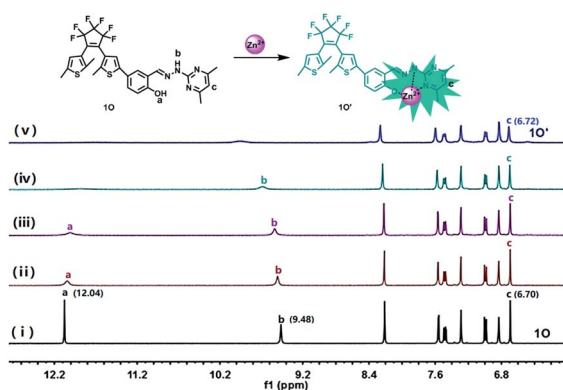

Fig. 6 ^1H NMR spectra (400 MHz) measured during the titration of **1O** with Zn^{2+} in CD_3CN. (i) free **1O**; (ii) **1O** + 0.2 equiv. of Zn^{2+}; (iii) **1O** + 0.4 equiv. of Zn^{2+}; (iv) **1O** + 0.6 equiv. of Zn^{2+}; (v) **1O** + 1.0 equiv. of Zn^{2+}.
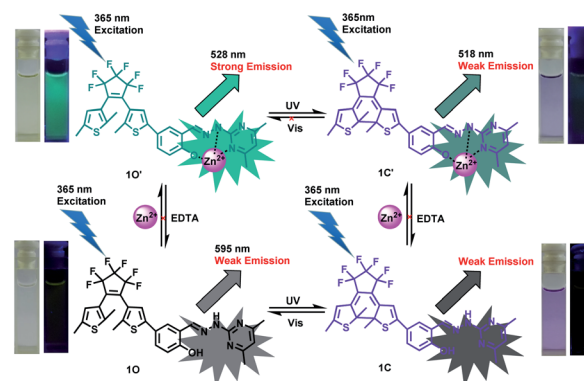

Fig. 7 Photochromism, color, and fluorescence changes of **1O** induced by Zn^{2+}/EDTA and UV/vis light.

sensor **1O** for Zn^{2+} detection, we investigated the fluorescence responses of sensor **1O** to Zn^{2+} in the presence of various competing metal ions (Fig. S8†). In the presence of Al^{3+}, Ca^{2+}, Sn^{2+}, K^+, Mg^{2+}, Cr^{3+}, Pb^{2+}, Hg^{2+}, Mn^{2+}, Fe^{3+}, Ag^+, Ba^{2+}, Cd^{2+}, and Sr^{2+}, there was small or no interference for Zn^{2+} detection, while Co^{2+}, Cu^{2+} and Ni^{2+} partially inhibited the emission intensity of the **1O**–Zn^{2+} complex. These experiments indicated that **1O** had high selectivity for Zn^{2+} detection as a fluorescence chemosensor.

The ^1H NMR analysis was initiated to demonstrate the binding interaction between sensor **1O** and Zn^{2+} in CD_3CN (Fig. 6). On addition of Zn^{2+}, the resonance signal of the –OH proton (H_a, 12.04) completely disappeared ultimately, suggesting that the O atom of –OH might coordinate to Zn^{2+}.[55] Besides, the –NH– (H_b, 9.48) signal of **1O** showed a significant downfield shift and declined gradually, which corresponded to the protonation of –NH–, suggesting the N–Zn^{2+} coordinate bond was formed. Meantime, the signal of hydrogen (H_c) on the pyrimidine shifted from 6.70 ppm to 6.72 ppm, suggesting that the N atom of the pyrimidine unit might coordinate to Zn^{2+}. These results indicated that the O atom on –OH and the N atoms on –NH– and the pyrimidine unit were the most probably binding sites. To further confirm the formation of the **1O**–Zn^{2+} complex, the ESI mass spectral analysis was also performed. As shown in Fig. S9,† the major peak at m/z 685.0577 was assigned to $[1O + Zn^{2+} + H^+]^+$ (calcd 685.0492), advocating a 1 : 1 bonding mode of **1O** with Zn^{2+}.

Application in logic circuit

The multi-responsive behaviors of sensor **1O** have been investigated under stimuli by Zn^{2+}/EDTA and ultraviolet/visible lights
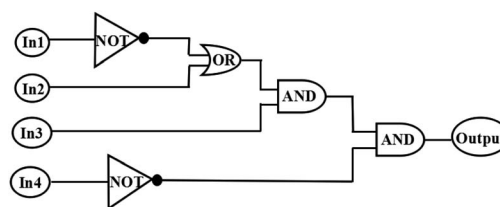

Fig. 8 The combinational logic circuits equivalent to the truth table given in Table 1: In1 (297 nm light), In2 ($\lambda > 500$ nm light), In3 (Zn^{2+}), In4 (EDTA) and output (strong fluorescence at 528 nm).

Table 1 Truth table for all possible strings of four binary-input data and the corresponding output digit[a]

Inputs				Output (λ_{em} = 528 nm)
In1 (UV)	In2 (vis)	In3 (Zn^{2+})	In4 (EDTA)	
0	0	0	0	0
0	0	0	1	0
0	0	1	0	1
0	1	1	0	1
0	1	1	1	1
1	0	0	0	0
1	1	0	0	0
1	1	1	0	1
1	0	1	0	0
1	0	0	1	0
1	0	1	1	0
1	1	1	1	1
1	1	0	1	0
0	1	0	1	0
0	0	1	1	1
0	1	0	0	0

[a] When the emission intensity at 528 nm more than 5-folds of the original state, the output signal is defined as '1', otherwise defined as '0'.

(Fig. 7). Therefore, an idealized logic circuit consisting of four input signals (ultraviolet light works as In1, visible lights works as In2, Zn^{2+} works as In3 and EDTA works as In4) and one output signal (the fluorescence emission intensity at 528 nm) was designed (Fig. 8). The four input signals in the logic circuit could be either 'on' or 'off' state, corresponding to the different Boolean values of '1' or '0'. When 297 nm ultraviolet light was employed, In1 was assigned as '1' corresponding to the 'on' states of the readout signals. Likewise, In2 was assigned as '1' by irradiation with visible light (λ > 500 nm), In3 was assigned as '1' when Zn^{2+} was added and In4 was assigned as '1' when EDTA was added. The emission intensity of **1O** at 528 nm was considered to be the original value. When the emission intensity at 528 nm was 5 folds greater than the original value, the output signal could serve as '1' corresponding to the 'on' states of the readout signals. If not, it was defined as an 'off' state. According to the Fig. 7, all possible logic strings were derived in the logic circuit (Fig. 8) and the corresponding truth table is listed in Table 1.[56,57]

Conclusions

In this work, a new type of multi-responsive fluorescence sensor based on a diarylethene derivative with a 4,6-dimethylpyrimidine unit was developed. The sensor was highly selective and sensitive toward Zn^{2+} with a lower limit of detection (8.48 × 10^{-8} mol L^{-1}). Furthermore, an integrated circuit with multiple control switches was successfully constructed based on its multiple stimuli-responsive fluorescence switching behavior. All results provided a useful strategy for the construction of new fluorescent chemosensors based on diarylethenes for the recognition of specific metal ions in the future.

Conflicts of interest

There are no conflicts of interest to declare.

Acknowledgements

Notes and references

1 D. Wu, A. C. Sedgwick, T. Gunnlaugsson, E. U. Akkaya, J. Y. Yoon and T. D. James, *Chem. Soc. Rev.*, 2017, **46**, 7105–7123.

2 G. Sivaraman, M. Iniya, T. Anand, N. G. Kotla, O. Sunnapu, S. Singaravadivel, A. Gulyani and D. Chellappa, *Coord. Chem. Rev.*, 2018, **357**, 50–104.

3 A. Gupta and N. Kumar, *RSC Adv.*, 2016, **6**, 106413–106434.

4 J. Q. Sun, B. F. Ye, G. M. Xia and H. M. Wang, *Sens. Actuators, B*, 2017, **249**, 386–394.

5 X. Q. Chen, T. Pradhan, F. Wang, J. S. Kim and J. Y. Yoon, *Chem. Rev.*, 2012, **112**, 1910–1956.

6 M. Saleem and K. H. Lee, *RSC Adv.*, 2015, **5**, 72150–72287.

7 J. F. Li, C. X. Yin and F. J. Huo, *Dyes Pigm.*, 2016, **131**, 100–133.

8 G. T. Sfrazzetto, C. Satriano, G. A. Tomaselli and E. Rizzarelli, *Coord. Chem. Rev.*, 2016, **311**, 125–167.

9 R. Singh, A. Gogoi and G. Das, *RSC Adv.*, 2016, **6**, 112246–112252.

10 S. B. Roy, J. Mondal, A. R. Khudabukhsh and K. K. Rajak, *New J. Chem.*, 2016, **40**, 9593–9608.

11 C. Kar, S. Samanta, S. Mukherjee, B. K. Datta, A. Ramesh and G. Das, *New J. Chem.*, 2014, **38**, 2660–2669.

12 P. S. Addy, S. B. Roy, S. M. Mandal and A. Basak, *RSC Adv.*, 2014, **4**, 23314–23318.

13 K. Du, S. Z. Niu, L. Qiao, Y. D. Dou, Q. Zhu, X. Z. Chen and P. F. Zhang, *RSC Adv.*, 2017, **7**, 40615–40620.

14 A. Mandal, A. Maity, S. Bag, P. Bhattacharya, A. K. Das and A. Basak, *RSC Adv.*, 2017, **7**, 7163–7169.

15 R. B. Cole, *Anal. Chem.*, 2011, **79**, 5510–5520.

16 J. P. Jiang and Z. J. Guo, *Coord. Chem. Rev.*, 2004, **248**, 205–229.

17 E. M. Nolan and S. J. Lippard, *Acc. Chem. Res.*, 2009, **42**, 193–203.

18 L. L. Zhang, J. Cao, K. Chen, Y. Liu, Y. S. Ge, J. Wu and D. Liu, *New J. Chem.*, 2019, **43**, 3071–3077.

19 J. Cao, C. C. Zhao, X. Z. Wang, Y. F. Zhang and W. H. Zhu, *Chem. Commun.*, 2012, **48**, 9897–9899.

20 Y. Mikata, S. Takeuchi, H. Konno, S. Iwatsuki, S. Akaji, I. Hamagami, M. Aoyama, K. Yasuda, S. Tamotsu and S. C. Burdette, *Dalton Trans.*, 2014, **43**, 10013–10022.

21 L. Y. Zhao, Q. L. Mi, G. K. Wang, J. H. Chen, J. F. Zhang, Q. H. Zhao and Y. Zhou, *Tetrahedron Lett.*, 2013, **54**, 3353–3358.

22 L. Fan, J. C. Qin, T. R. Li, B. D. Wang and Z. Y. Yang, *Sens. Actuators, B*, 2014, **203**, 550–556.

23 Z. Kowser, H. Tomiyasu, X. Jiang, U. Rayhan, C. Redshaw and T. Yamato, *New J. Chem.*, 2015, **39**, 4055–4062.

24 B. Zhang, K. S. Cao, Z. A. Xu, Z. Q. Yang, H. W. Chen, W. Huang, G. Yin and X. Z. You, *Eur. J. Inorg. Chem.*, 2012, **2012**, 3844–3851.

25 K. Komatsu, Y. Urano, H. Kojima and T. Nagano, *J. Am. Chem. Soc.*, 2008, **130**, 14533–14543.

26 X. D. Zhang, H. Li, G. Liu and S. Z. Pu, *J. Photochem. Photobiol., A*, 2016, **330**, 22–29.

27 S. J. Xia, G. Liu and S. Z. Pu, *J. Mater. Chem. C*, 2015, **3**, 4023–4029.

28 Z. Wang, S. Q. Cui, S. Y. Qiu and S. Z. Pu, *J. Photochem. Photobiol., A*, 2019, **376**, 185–195.

29 Q. Luo, H. Cheng and H. Tian, *Polym. Chem.*, 2011, **2**, 2435–2443.

30 M. Morimoto, R. Kashihara, K. Mutoh, Y. Kobayashi, J. Abe, H. Sotome, S. Ito, H. Miyasakac and M. Irie, *Crystengcomm*, 2016, **18**, 7241–7248.

31 Y. Takagi, T. Kunishi, T. Katayama, Y. Ishibashi, H. Miyasaka, M. Morimoto and M. Irie, *Photochem. Photobiol. Sci.*, 2012, **11**, 1661–1665.

32 S. Z. Pu, Q. Sun, C. B. Fan, R. J. Wang and G. Liu, *J. Mater. Chem. C*, 2016, **4**, 3075–3093.

33 Z. C. Xu, J. Y. Yoon and D. R. Spring, *Chem. Commun.*, 2010, **46**, 2563–2565.

34 Y. Xu, J. Meng, L. Meng, Y. Dong, Y. Cheng and C. Zhu, *Chemistry*, 2010, **16**, 12898–12903.

35 X. J. Liu, N. Zhang, J. Zhou, T. J. Chang, C. L. Fang and D. H. Shangguan, *Analyst*, 2013, **138**, 901–906.

36 Y. Mikata, A. Yamashita, K. Kawata, H. Konno, S. Itami, K. Yasuda and S. Tamotsu, *Dalton Trans.*, 2011, **40**, 4976–4981.

37 A. Dhara, N. Guchhait, I. Mukherjee, A. Mukherjee and S. C. Bhattacharya, *RSC Adv.*, 2016, **6**, 105930–105939.

38 S. Z. Pu, Z. P. Tong, G. Liu and R. J. Wang, *J. Mater. Chem. C*, 2013, **31**, 4726–4739.

39 F. Shi, S. Q. Cui, H. L. Liu and S. Z. Pu, *Dyes Pigm.*, 2020, **173**, 107914.

40 A. Jana, B. Das, S. K. Mandal, S. Mabhai, A. R. Khuda-Bukhsh and S. Dey, *New J. Chem.*, 2016, **40**, 5976–5984.

41 Z. X. Li, L. Y. Liao, W. Sun, C. H. Xu, C. Zhang, C. J. Fang and C. H. Yan, *J. Phys. Chem. C*, 2008, **112**, 5190–5196.

42 S. Kawai, T. Nakashima, K. Atsumi, T. Sakai, M. Harigai, Y. Imamoto, H. Kamikubo, M. Kataoka and T. Kawai, *Chem. Mater.*, 2007, **19**, 3479–3483.

43 M. Morimoto and M. Irie, *Chemistry*, 2006, **12**, 4275–4282.

44 T. Nakashima, K. Miyamura, T. Sakai and T. Kawai, *Chemistry*, 2009, **15**, 1977–1984.

45 S. Wang, W. Shen, Y. Feng and H. Tian, *Chem. Commun.*, 2006, **14**, 1497–1499.

46 S. Irie, M. S. Kim, T. Kawai and M. Irie, *Bull. Chem. Soc. Jpn.*, 2004, **77**, 1037–1040.

47 S. Z. Pu, G. Liu, L. Shen and J. K. Xu, *Org. Lett.*, 2007, **9**, 2139–2142.

48 T. Kawai, M. S. Kim, T. Sasaki and M. Irie, *Opt. Mater.*, 2003, **21**, 275–278.

49 Z. Wang, S. Q. Cui, S. Y. Qiu and S. Z. Pu, *RSC Adv.*, 2018, **8**, 29295–29300.

50 R. J. Wang, L. Diao, Q. W. Ren, G. Liu and S. Z. Pu, *ACS Omega*, 2019, **4**, 309–319.

51 J. H. Cheng, X. G. Zhou and H. F. Xiang, *Analyst*, 2015, **140**, 7082–7115.

52 J. S. Wu, W. M. Liu and X. Q. Zhuang, *Org. Lett.*, 2007, **9**, 33–36.

53 Y. W. Wang, M. X. Yu, Y. H. Yu, Z. P. Bai, Z. Shen, F. Y. Li and X. Z. You, *Tetrahedron Lett.*, 2009, **50**, 6169–6172.

54 S. Y. Tao, Y. Wei, C. Wang, Z. Q. Wang, P. Fan, D. Shi, B. J. Ding and J. S. Qiu, *RSC Adv.*, 2014, **4**, 46955–46961.

55 S. H. Xiao, Z. Liu, J. Y. Zhao, M. S. Pei, G. Y. Zhang and W. He, *RSC Adv.*, 2016, **6**, 27119–27125.

56 Z. Wang, S. Q. Cui, S. Y. Qiu and S. Z. Pu, *J. Photochem. Photobiol., A*, 2018, **367**, 212–218.

57 S. Wang, L. L. Ma, G. Liu and S. Z. Pu, *Dyes Pigm.*, 2019, **164**, 257–266.